


## ORIGINAL ARTICLE

# m6A modification-mediated lncRNA TP53TG1 inhibits gastric cancer progression by regulating CIP2A stability

Deliang Fang<sup>1,2</sup> | Xinde Ou<sup>1,2</sup> | Kaiyu Sun<sup>1</sup> | Xingyu Zhou<sup>1,2</sup> | Youpei Li<sup>3</sup> | Peng Shi<sup>4</sup> | Zirui Zhao<sup>1,2</sup> | Yulong He<sup>1,5</sup> | Jianjun Peng<sup>1</sup> | Jianbo Xu<sup>1</sup> 

<sup>1</sup>Department of Gastrointestinal Surgery, The First Affiliated Hospital, Sun Yat-sen University, Guangzhou, China

<sup>2</sup>Laboratory of General Surgery, The First Affiliated Hospital, Sun Yat-sen University, Guangzhou, China

<sup>3</sup>Department of Anesthesiology, Sun Yat-sen Memorial Hospital, Sun Yat-sen University, Guangzhou, China

<sup>4</sup>Huazhong University of Science and Technology Union Shenzhen Hospital, Shenzhen, China

<sup>5</sup>Digestive Disease Center, The Seventh Affiliated Hospital, Sun Yat-sen University, Shenzhen, China

## Correspondence

Jianjun Peng and Jianbo Xu, Department of Gastrointestinal Surgery, The First Affiliated Hospital, Sun Yat-sen University, No. 58 Zhongshan 2nd Road, Guangzhou 510080, China.

Emails: [pjianj@mail.sysu.edu.cn](mailto:pjianj@mail.sysu.edu.cn); [xjianb@mail.sysu.edu.cn](mailto:xjianb@mail.sysu.edu.cn)

## Funding information

National Natural Science Foundation of China, Grant/Award Number: 81871915 and 81672343; Natural Science Foundation of Guangdong, China, Grant/Award Number: 2022A1515012140, 2017A030313570 and 2018A030313543

## Abstract

Long noncoding RNAs (lncRNAs) are associated with various types of cancer. However, the precise roles of many lncRNAs in tumor progression remain unclear. In this study, we found that the expression of the lncRNA TP53TG1 was downregulated in gastric cancer (GC) and it functioned as a tumor suppressor. In addition, low TP53TG1 expression was significantly associated with poor survival in patients with GC. TP53TG1 inhibited the proliferation, metastasis, and cell cycle progression of GC cells, while it promoted their apoptosis. m6A modification sites are highly abundant on TP53TG1, and demethylase ALKBH5 reduces TP53TG1 stability and downregulates its expression. TP53TG1 interacts with cancerous inhibitor of protein phosphatase 2A (CIP2A) and triggers its ubiquitination-mediated degradation, resulting in the inhibition of the PI3K/AKT pathway. These results suggest that TP53TG1 plays an important role in inhibiting the progression of GC and provides a crucial target for GC treatment.

## KEYWORDS

ALKBH5, CIP2A, gastric cancer, PI3K/AKT, TP53TG1

## 1 | INTRODUCTION

Gastric cancer (GC) has become a continuous and major global health problem, and GC was the fifth most frequent cause of cancer-related

death in 2020.<sup>1</sup> The latest statistics from the Chinese National Cancer Center showed that the incidence rate of GC ranks second<sup>2</sup> among malignant tumors, largely due to high rates of *Helicobacter pylori* infection.<sup>3</sup> In particular, most GC patients are diagnosed in

**Abbreviations:** CCK-8, cell-counting kit 8; CHIRP, chromatin isolation by RNA purification; CHX, cycloheximide; CIP2A, cancerous inhibitor of protein phosphatase 2A; GC, gastric cancer; RIP, RNA immunoprecipitation; RT-qPCR, reverse-transcription quantitative PCR; TP53TG1, TP53 target 1.

Deliang Fang, Xinde Ou, and Kaiyu Sun have contributed equally to this work and share first authorship.

This is an open access article under the terms of the [Creative Commons Attribution-NonCommercial](https://creativecommons.org/licenses/by-nc/4.0/) License, which permits use, distribution and reproduction in any medium, provided the original work is properly cited and is not used for commercial purposes.

© 2022 The Authors. *Cancer Science* published by John Wiley & Sons Australia, Ltd on behalf of Japanese Cancer Association.

the middle or advanced stages and receive a dismal prognosis.<sup>4</sup> Therefore, discovering new biomarkers at the molecular level for early diagnosis, tumor grading, and prognosis of GC is a critical need.

Long noncoding RNAs (lncRNAs), a class of functional noncoding RNA transcripts >200 nt in length, are key regulators of GC occurrence, development, metastasis, and GC cell escape from the immune system.<sup>5,6</sup> lncRNAs can regulate gene expression by regulating epigenetic modifications, transcription, and posttranscriptional events.<sup>7-9</sup> The association between lncRNAs and GC development has been established based on multiple studies. For example, the lncRNA HNF1A-AS1 promotes GC cell proliferation and cell cycle progression by enhancing the expression of cell cycle regulators and promoting p21 ubiquitination-mediated degradation.<sup>10</sup> In addition, under metabolic stress, MACC1-AS1 enhances GC cell glycolysis and antioxidant activity through increased AMPK/Lin28-mediated MACC1 mRNA stability.<sup>11</sup> Most studies have focused on lncRNAs that play roles in promoting GC progression. But lncRNAs that function as a tumor suppressor also play an important role in GC. Thus, we focused on the lncRNAs that play a tumor suppressor role in GC.

The N<sup>6</sup>-methyladenosine (m<sup>6</sup>A) methylation modification is the most common lncRNA modification and acts as a critical upstream regulatory mechanism of lncRNAs.<sup>12</sup> In cancers, a m<sup>6</sup>A methyltransferase catalyzes the methylation of oncogene/suppressor RNA, and then a series of m<sup>6</sup>A reader proteins recognize these m<sup>6</sup>A modifications, leading to upregulated or downregulated oncogene/suppressor gene expression.<sup>13</sup> m<sup>6</sup>A modification is highly prevalent in GC, and its dynamic regulation has been shown to be significantly correlated with gene expression.<sup>14,15</sup> ARHGAP5-AS1 stimulates the m<sup>6</sup>A modification of ARHGAP5 in the cytoplasm by recruiting METTL3 to promote GC progression.<sup>16</sup> ALKBH5 promotes GC cell invasion and metastasis by demethylating the lncRNA NEAT1.<sup>17</sup> Thus, m<sup>6</sup>A-mediated regulation might greatly influence GC progression.

In this study, we reveal that TP53TG1 inhibits the progression of GC by interacting with cancerous inhibitor of protein phosphatase 2A (CIP2A) and triggering its ubiquitination-mediated degradation. In addition, we explored a new mechanism of TP53TG1 downregulation mediated by m<sup>6</sup>A modification in GC. The results demonstrate that TP53TG1 is a tumor suppressor, which may serve as a crucial marker of GC prognosis and may be a promising therapeutic target.

## 2 | MATERIALS AND METHODS

### 2.1 | Tissue samples

A total of 82 matched normal and cancer tissues were collected from 82 patients with GC who were diagnosed at the First Affiliated Hospital of Sun Yat-sen University and underwent radical excision between January 2012 and December 2017. Patients who died within 3 months after surgery or had more than one primary tumor were excluded. None of the patients had received preoperative chemotherapy or radiotherapy. All tissue specimens were separated and frozen at -80°C or formalin fixed and paraffin embedded.

Experienced pathologists from the First Affiliated Hospital of Sun Yat-sen University reviewed the tissue sections. Written and informed consent was obtained from all patients. The study followed the guidelines of the Ethics Committee of the First Affiliated Hospital of Sun Yat-sen University.

### 2.2 | Immunohistochemistry (IHC)

Sample slides were deparaffinized, rehydrated, and subjected to antigen retrieval; endogenous peroxidase activities were blocked. Slides were then incubated at 4°C overnight in the indicated antibodies, including those against CIP2A (1:200; ab99518, Abcam), PP2A (1:200; Merck), Ki67 (1:200; 12202S, CST), and BAX (1:200; 5023S, CST). Then, the slides were incubated with a horseradish peroxidase-conjugated secondary antibody and DAB and counterstained with hematoxylin. Images were obtained with confocal laser scanning microscope (Zeiss) and processed using the ZEN imaging software. IHC scoring of tissue sections was performed as described previously.<sup>18</sup>

### 2.3 | Cell culture

The GC cell lines AGS, MKN28, BGC823, HCG27, MGC803, and MKN45 were derived from the Type Culture Collection of the Chinese Academy of Sciences. The normal gastric epithelial cell line GES-1 was obtained from the Lab Animal Center of the Fourth Military Medical University. MKN28, HCG27, MGC803, and MKN45 were cultured in DMEM (Invitrogen). BGC823 was cultured in RPMI-1640 (Invitrogen), and AGS was cultured in F12 (Invitrogen). All cell lines were supplemented with 10% fetal bovine serum (GIBCO) in an incubator with 5% CO<sub>2</sub> and 95% room air at 37°C. The cell lines were tested for potential mycoplasma contamination by PCR using a MycoGuard™ Mycoplasma PCR detection kit (GeneCopoeia) and were confirmed mycoplasma negative.

### 2.4 | Lentivirus construction and cell transfection

Packaging vectors pSPAX2 and pMD2.0G were, respectively, cotransfected with overexpression or knockdown of stable transfection vector plasmids into HEK293T cells using Lipofectamine 3000 (Invitrogen). After 16 hours of transfection, the medium of HEK293T cells was removed and replaced with fresh culture medium. After 48 hours, the cell supernatant was filtered and collected with 0.22-micron filter membrane. Then, the GC cell lines were infected with the corresponding recombinant lentivirus for 48 hours and subsequently selected with 2 µg/ml puromycin for 2 weeks.

TP53TG1 gene, ALKBH5 gene, and CIP2A gene were cloned into the pEZ-Lv201 lentivirus vector (GeneCopoeia), while the corresponding vector pEZ-Lv201 (EGFP, a reporter gene) was used as a control vector.

Lentiviral shRNA constructs were obtained from GeneCopoeia (GeneCopoeia). The lentiviral shRNA control plasmid was added with a scrambled control sequence (ACAGAAGCGATTGTTGATC), which was basically mismatched. The targeting sequences were as follows: Lv201-shTP53TG1#1 GCATCAGCTGATGATGACAGC, Lv201-shTP53TG1#2 GCAGGAAGCGATGGTTAAGAC; Lv201-shALKBH5#1 GAAAGGCTGTTGGCATCAATA, Lv201-shALKBH5#2 CCTCAGGAAGACAAGATTAGA.

## 2.5 | Immunofluorescence in situ hybridization (FISH)

Cy3-labeled TP53TG1 probe was designed and synthesized by the GenePharma Fluorescent in Situ Hybridization Kit (GenePharma). For FISH assay, AGS or MKN28 cells ( $3 \times 10^5$  cells) were fixed in 4% formaldehyde and permeabilized with 0.3% Triton X-100 for 15 minutes and washed three times with PBS and once in  $2 \times$  SSC buffer. Hybridization was carried out using Cy3-labeled TP53TG1 probe sets at 37°C for 16 hours. Images were obtained with a confocal laser scanning microscope (Zeiss) and processed using the ZEN imaging software. TP53TG1 probes are listed in Table S1.

## 2.6 | Reverse-transcription quantitative PCR (RTqPCR)

An RNA isolation plus kit (TaKaRa) was used to extract total RNA from GC tissues or cells. After reverse transcription with Primer Script<sup>TM</sup> RT Reagent (TaKaRa), cDNAs were harvested and then subjected to real-time PCR analysis with a SYBR green detection system (TaKaRa) with an ABI 7900HT instrument (Applied Biosystems); the amplification cycle of qualitative RT-PCR was 35. GAPDH was used as the endogenous control. The primers used for the qPCR analysis are listed in Table S1.

## 2.7 | Chromatin isolation by RNA purification

We designed the probes for CHIRP (one probe per 100 nt of RNA). The probes were biotin-labeled DNA probes that were complementary to the target RNA sequence. TP53TG1 probes used for CHIRP are listed in Table S1. RNA was extracted from AGS cells or transcribed in vitro and purified. Then, the purified RNA was pre-immunoprecipitated with specific prewashed beads at 37°C for 30 minutes. After centrifugation, the supernatant was retained. Subsequently, the supernatant was hybridized with denatured biotin-labeled RNA probes at 55°C for 2 hours. Next, the prewashed beads were added, rotated at 37°C for 1 hour, and centrifuged at 3000g for 30 seconds. The supernatant was discarded, and the beads were washed five to six times. Separation buffer was used to elute RNA and protein sequentially. Then, the protein from the complex was subjected to immunoblot assay and liquid chromatography

(LC)/mass spectrometry (MS) assay, and the RNA complexes were purified with TRIzol reagent and then subjected to RT-qPCR analysis.

## 2.8 | RNA immunoprecipitation (RIP)

RNA immunoprecipitation assays were carried out using a Magna RIP RNA-binding protein immunoprecipitation kit (Millipore) according to the manufacturer's instructions. Anti-CIP2A (Abcam) and normal rabbit IgG (CST) were used to immunoprecipitate target RNA or as the negative control. Finally, RT-qPCR analysis was performed to detect the enrichment of the coprecipitated RNA binding to CIP2A.

## 2.9 | Western blotting analysis

Total proteins were extracted using RIPA supplemented with protease and phosphatase inhibitor reagents (Thermo-Fisher Scientific). Equal amounts of protein samples were separated by SDS/PAGE and then transferred to PVDF membranes (Millipore). Next, the membranes were probed with specific primary antibodies at 4°C overnight (Table S2). After incubating with the secondary antibody, immunoreactive bands were visualized with enhanced chemiluminescence reagents (Bio-Rad).

## 2.10 | In vivo assays

Firstly, Lv201-TP53TG1 or control vector was stably transfected into BGC823 cells. Then, nude mice were injected in the axilla with 100  $\mu$ l ( $5 \times 10^7$  cells/ml) of the cell suspension containing the overexpression group or the NC group cells. The length and diameter of the subcutaneous tumors were measured and recorded, and their growth curves were drawn. Four and a half weeks after the tumor cell inoculation, the nude mice were sacrificed by cervical dislocation. The subcutaneous tumor was removed, measured, weighed, and photographed. Specimens were fixed with formalin solution and then sectioned and stained. In the lung metastasis model, 100  $\mu$ l ( $1 \times 10^7$  cells/ml) of the suspension with control or TP53TG1-overexpressing BGC823 cells was injected into the tail vein. After sacrifice, the lung specimens were separated and photographed, and the measurements were recorded. The lung specimens were fixed with formalin solution, sliced, and stained with HE; then, the number of metastatic nodules in each field of view was counted.

## 2.11 | Methylated RIP

Cells in 150-mm dishes were crosslinked by UV ( $4000 \times 100 \mu$ J/cm<sup>2</sup>, twice; Spectronics) and collected in PBS. The RNA-m6A complexes were isolated using 500  $\mu$ l of MeRIP buffer (150 mM NaCl; 10 mM Tris-HCl, pH 7.5; and 0.1% NP-40) and centrifuged at 21,000g for 5 minutes at 4°C. Then, the supernatant was collected in other

enzyme-free tubes, added to 5 µg anti-m6A (Synaptic System) or anti-IgG (Proteintech), and incubated overnight at 4°C. Incubated lysates containing antibody-protein-RNA complex with protein A/G magnetic beads (Thermo Fisher Scientific) were rotated for 1 hour at 4°C. Subsequently, the beads were collected and washed twice with wash buffer (0.1% SDS and 0.5% NP-40 in PBS). The RNA-m6A complex was de-crosslinked by heating at 45°C for 1 hour. Finally, the beads were extracted from cells using TRIzol (Thermo-Fisher) for RNA isolation, and RT-qPCR analysis was performed to detect the enrichment.

## 2.12 | RNA stability

For RNA stability measurements, GC cells were administered actinomycin D (Act-D, 5 µg/ml). After incubation, the cells were collected at the indicated times (0, 2, 4, 6, 8, or 16 hours). RNA was extracted using TRIzol reagent, and reverse-transcription was performed to detect the remaining mRNA using RT-qPCR.

## 2.13 | Statistical analysis

All data are presented as the mean ± standard deviation. Appropriate statistical methods including Student's *t* test, Wilcoxon signed-rank test, Mann-Whitney test, and Pearson chi-square test were used to calculate differences between groups. *P* values <0.05 indicate statistical significance. Statistical analyses were performed using SPSS Statistics software (version 18.0) or GraphPad Prism 8 software.

# 3 | RESULTS

## 3.1 | TP53TG1 is downregulated in GC and inversely associated with patient prognosis

To investigate the role of lncRNAs in GC, we first examined lncRNA expression profiles in three GC tissue samples and adjacent normal tissues by RNA sequencing. Among the differentially expressed lncRNAs, 82 were significantly upregulated, while 136 were significantly downregulated in GC tissues compared with the noncancerous tissues (fold change >2, *p* < 0.05, Figure S1A). Among them, TP53TG1 was the most significantly downregulated lncRNA in GC tissues compared with normal tissues (Figure 1A). By using an independent panel of 82 GC tissues and adjacent normal tissues, we found that TP53TG1 expression was downregulated in GC (Figure 1B), which was also confirmed by agarose gel electrophoresis assays (Figure 1C). More importantly, low TP53TG1 expression was associated with more advanced clinical features such as tumor diameter, differentiation, TNM categories, and lymph node metastasis stage. We also found that lower TP53TG1 expression was significantly correlated with worse prognosis in GC patients (Figure 1D, Table 1). The Kaplan-Meier plotter (<http://www.kmplot.com/>) was used to assess

the correlation between TP53TG1 and GC patients' survival, and the results further confirmed the above finding (Figure 1E). These results suggest that TP53TG1 can be used as a potential index for the early diagnosis and prognosis of GC. In addition, RT-qPCR revealed significantly lower levels of TP53TG1 expression in GC cells (Figure 1F). To investigate the cellular location of TP53TG1, RT-qPCR of the nuclear and cytoplasmic fractions of GC cells was conducted, which revealed that TP53TG1 was mainly localized in the cytoplasm (Figure 1G). FISH assay further confirmed that TP53TG1 located primarily in the cytoplasm in GC cells (Figure 1H).

## 3.2 | TP53TG1 functions as a tumor suppressor in vitro

To determine the physiological role of TP53TG1 in cancer, we stably overexpressed TP53TG1 in MKN28 and BGC823 cells and knocked it down in AGS cells (Figure 2A). With CCK-8, EdU assays, and colony formation, we found that ectopic expression of TP53TG1 inhibited MKN28 and BGC823 cell proliferation, while knockdown of TP53TG1 promoted the proliferation of AGS cells (Figure 2B–D, Figure S2A–C). Overexpression of TP53TG1 reproducibly resulted in cell cycle redistribution with a significant increase in the number of synchronized MKN28 and BGC823 cells in the G0/G1 phase and a significant decrease in these cells in other cell cycle stages. Moreover, depletion of TP53TG1 promoted cell cycle progression (Figure 2E, Figure S2D,F).

We found that TP53TG1 overexpression induced higher early apoptosis and late apoptosis rates, as measured by annexin-V and propidium iodide (PI) staining, whereas depletion of TP53TG1 decreased the apoptosis rate of AGS cells (Figure 2F, Figure S2E,G). Importantly, we observed that TP53TG1 attenuated GC cell migration and invasion (Figure 2G,H, Figure S2H,I). The epithelial-mesenchymal transition (EMT) process is one of the major causes of cell invasion and migration.<sup>19</sup> We then detected key EMT markers and found that N-cadherin, Vimentin, and Slug were all downregulated, while E-cadherin was upregulated when TP53TG1 was overexpressed. Knockdown of TP53TG1 significantly promoted EMT by leading to an opposite change of these markers (Figure 2I, Figure S3A,B). Together, our results demonstrate that TP53TG1 is involved in tumor progression, specifically suggesting that TP53TG1 performs a critical tumor-suppressing function in GC progression.

To explore the downstream signaling pathways in which TP53TG1 is involved, we performed mRNA sequencing and subsequent bioinformatic analysis with MKN28 cells treated with an empty vector or TP53TG1 overexpression vector. Kyoto Encyclopedia of Genes and Genomes (KEGG) enrichment analysis indicated that TP53TG1 was correlated with PI3K/AKT pathways directly involved in the regulation of the cell cycle, apoptosis, and cell migration (Figure S1B,C). By analyzing the activities of the PI3K/AKT pathway in GC cells, we found that TP53TG1 overexpression reduced AKT Thr308 and Ser473 phosphorylation, while TP53TG1 knockdown increased phosphorylation at these sites (Figure 2J).

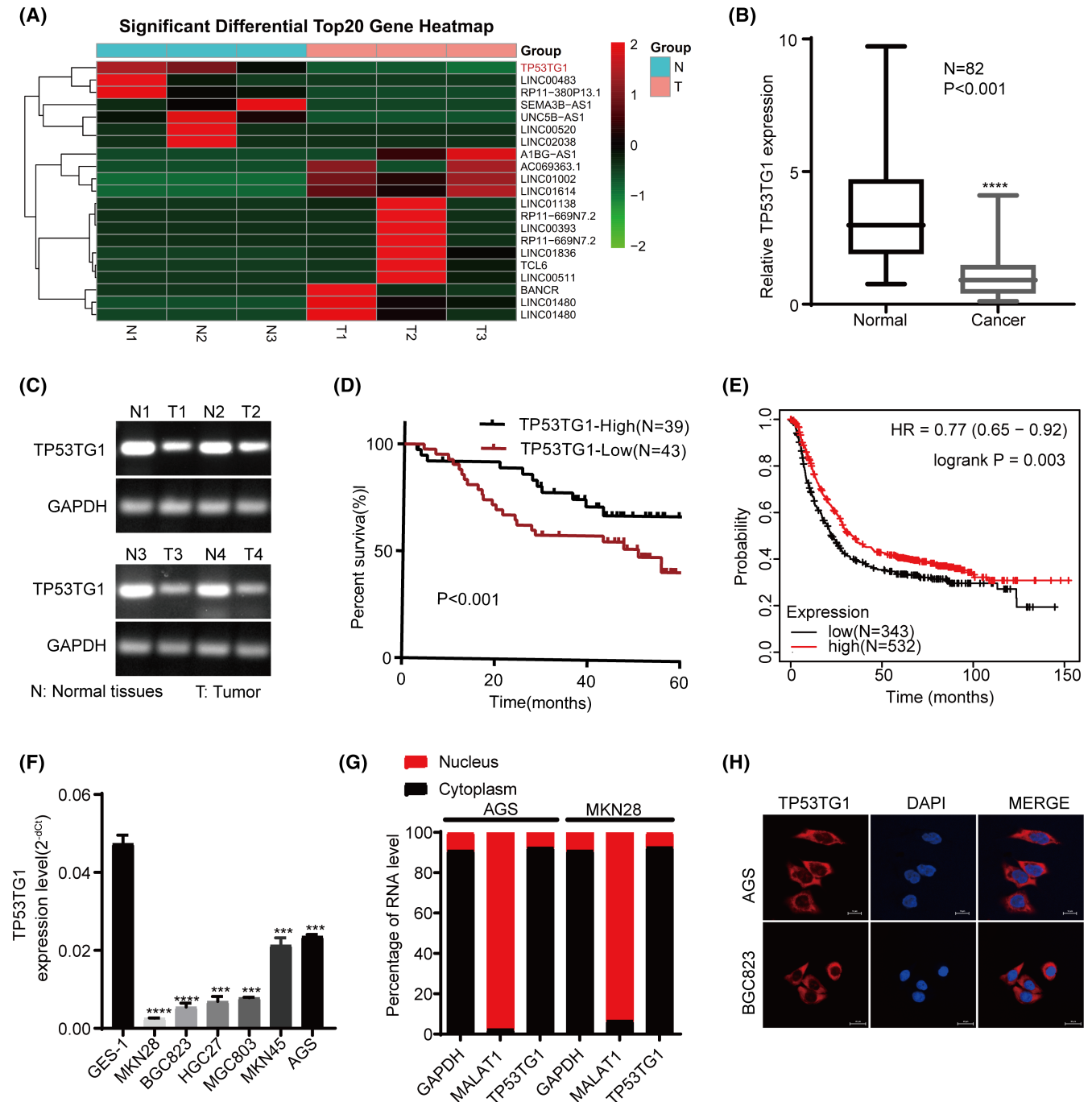


**FIGURE 1** TP53TG1 expression was downregulated in gastric cancer (GC), and it was primarily located in the cytoplasm. (A) Heatmap showing candidate RNA sequences in GC and paired normal tissues. (B) RT-qPCR results showing the decreased expression of TP53TG1 in 82 paired GC and adjacent normal gastric tissue samples. (C) Agarose gel electrophoresis assays revealed that the level of TP53TG1 was significantly decreased in GC. (D) Survival curve of TP53TG1-low-expression and TP53TG1-high-expression groups. Median relative TP53TG1 expression value (1.122) was used to divide patients into TP53TG1-high and TP53TG1-low groups. (E) Kaplan-Meier analysis revealed that GC patients with lower TP53TG1 expression had a dismal prognosis. (F) TP53TG1 expression levels in GES-1 cells and GC lines. (G, H), Nucleocytoplasmic separation experiment and RNA immuno-FISH revealing the subcellular location of TP53TG1 in GC cells.

### 3.3 | TP53TG1 interacts with CIP2A and triggers its ubiquitination-mediated degradation

To investigate the potential mechanism underlying the biological functions of TP53TG1, we designed and synthesized specific

TP53TG1 probes to perform CHIRP assay and subsequent MS analysis (Figure 3A). The MS results showed that the key cancer-promoting protein CIP2A has a high abundance (Figure S1D). CIP2A is reported to be an upstream inhibitor of the PI3K/AKT signaling pathway by inhibiting PP2A activity.<sup>17</sup> To further confirm the

Parameters	Number of cases	TP53TG1 expression		P value
		Low (43)	High (39)	
Sex				
Male	55	26	29	0.18117
Female	27	17	10	
Age				
<60	40	22	18	0.65071
≥60	42	21	21	
Tumor size				
≤4 cm	42	14	28	0.00039***
>4 cm	40	29	11	
Primary tumor (T) stage				
T1-T2	29	7	21	0.00034***
T3-T4	54	36	18	
Lymph node metastasis				
Yes	58	35	23	0.02585**
No	24	8	16	
Distant metastasis				
Yes	22	17	5	0.0064**
No	60	26	34	
TNM stage				
I/II	34	11	23	0.0022**
III/IV	48	32	16	

The pathological diagnoses and classifications were made according to Ref.<sup>44</sup>

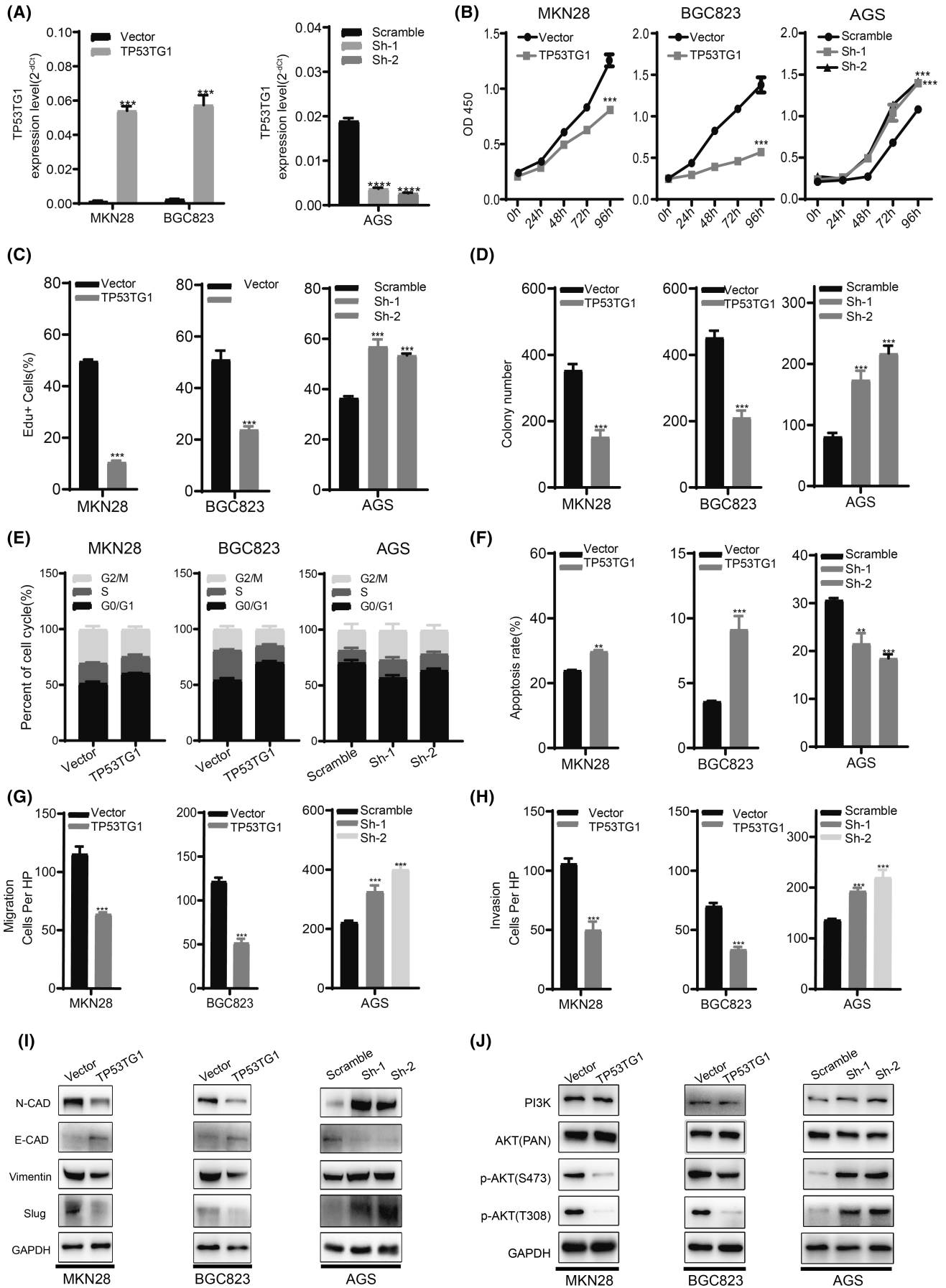
\*\* $p < 0.01$ ; \*\*\* $p < 0.001$ .

interaction between TP53TG1 and CIP2A, we carried out Western blot analysis with CHIRP assay and found that the CIP2A was pulled down by TP53TG1 (Figure 3B). Furthermore, we conducted RIP experiment and discovered that compared with the IgG control, the anti-CIP2A antibody bound with higher abundance to TP53TG1 in GC cells (Figure 3C). These findings indicated a direct binding between TP53TG1 and CIP2A. We further analyzed the expression of CIP2A when the TP53TG1 level was changed and found that the protein level of CIP2A was significantly reduced when TP53TG1 was overexpressed (Figure 3D), while it was significantly increased when TP53TG1 was knocked down (Figure S2J). In addition, IF staining showed lower levels of the CIP2A protein in TP53TG1-overexpressing GC cells than in control cells (Figure 3E), while higher levels of the CIP2A protein were observed in TP53TG1-knockdown AGS cells than in control cells (Figure S2K). However, we found no difference in the mRNA level of CIP2A when TP53TG1 was changed

(Figure 3F). In addition, IHC staining combined with RT-qPCR analysis also revealed downregulated CIP2A expression in tissue samples with high TP53TG1 expression (Figure 3G).

According to these findings, we inferred that the stability of the CIP2A protein was diminished upon binding to TP53TG1, which meant that TP53TG1 promoted its degradation. Therefore, we conducted time-varying gradient stimulation experiments with the protein synthesis inhibitor imine cyclohexanone (CHX) and proteasome inhibitor (MG132) and found that when TP53TG1 was overexpressed, the CIP2A protein level decreased significantly, indicating that TP53TG1 promoted the degradation of the CIP2A protein (Figure 3H–J). Subsequent ubiquitination assays revealed that TP53TG1 overexpression increased the level of ubiquitinated CIP2A protein in MKN28 and BGC823 cells (Figure 3K). Taken together, we concluded that TP53TG1 can directly bind to CIP2A and promote its degradation.

**FIGURE 2** TP53TG1 inhibited cell proliferation and the PI3K/AKT pathway. (A) RT-qPCR analysis was conducted to detect TP53TG1 levels in stably transfected gastric cancer (GC) cells. (B) CCK-8 assay measured the effects of TP53TG1 on the proliferation of GC cells. (C, D) Statistical analysis of the EdU and colony formation assays are shown. (E) Statistical analysis of FACS showed that TP53TG1 affected cell cycle progression in GC cells. (F) Statistical analysis of apoptosis of GC cells. (G, H) Statistical analysis of the migration and invasion assays. (I) Western blotting was performed to detect levels of the key proteins of the epithelial-mesenchymal transition (EMT) process. (J) Western blotting was performed to detect the levels of the key proteins of the PI3K/AKT signaling pathway.



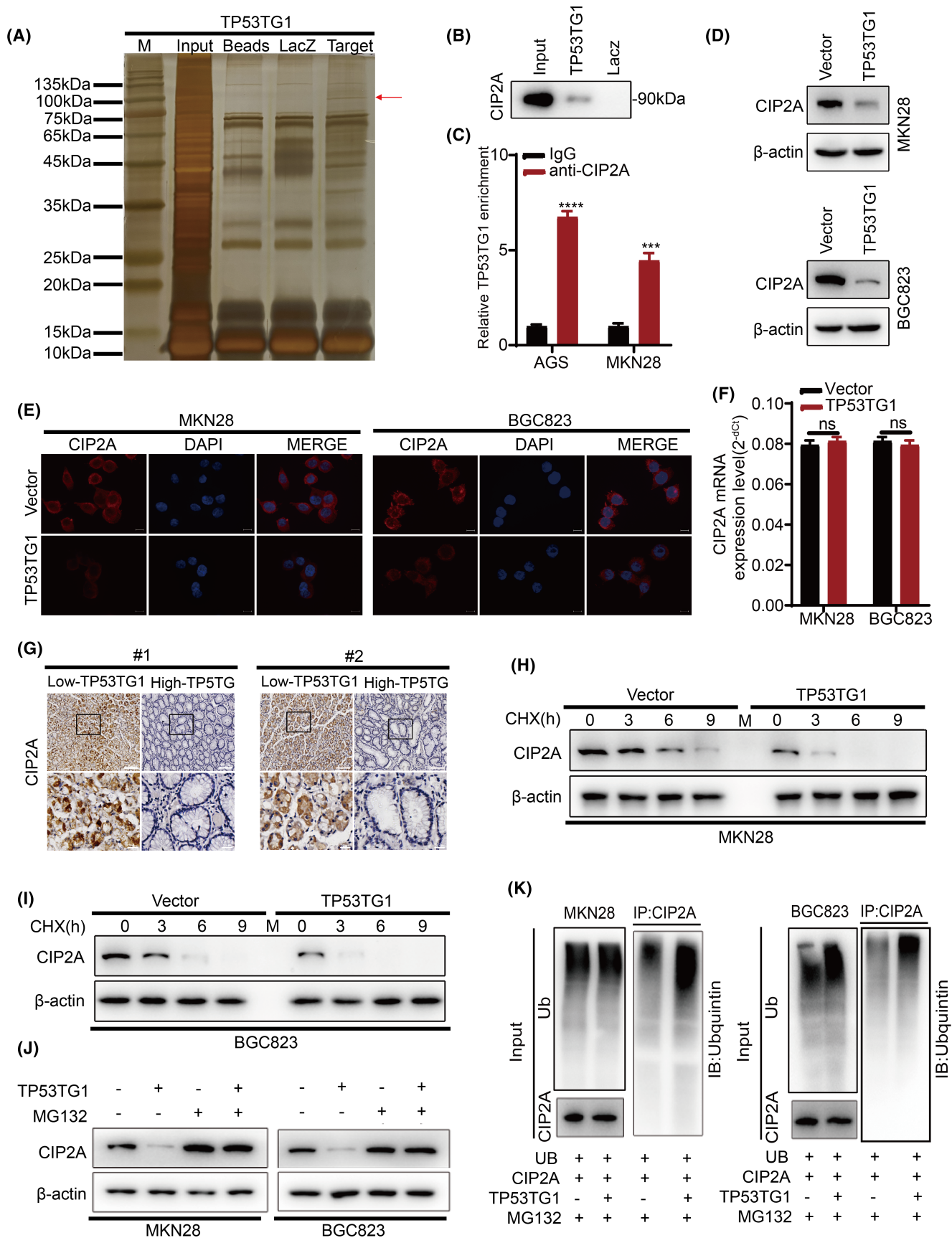




**FIGURE 3** TP53TG1 directly bound to CIP2A and triggered its ubiquitination-mediated degradation. (A) The pulled-down proteins were resolved on SDS-PAGE gels and visualized using silver staining. (B) Western blot analysis revealed the interaction between TP53TG1 and CIP2A in gastric cancer (GC) cell extracts. (C) RIP assay showing the levels of coprecipitated CIP2A mRNA. (D) Western blotting was used to analyze the levels of CIP2A in GC cells transfected with TP53TG1 or negative control (E) Representative images of immunofluorescence staining for CIP2A expression in TP53TG1-overexpressing or NC cells. (F) RT-qPCR analysis of CIP2A mRNA levels in TP53TG1-overexpressing or NC cells. (G) CIP2A protein expression in GC tissue with low or high TP53TG1 expression, as measured by immunohistochemistry (IHC). (H, I) CHX treatment was administered to assess CIP2A degradation in GC cells. (J) MG-132 abolished the downregulation of CIP2A protein expression induced by TP53TG1 overexpression in GC cells. (K) Ubiquitination assays revealed that TP53TG1 overexpression increased the level of the ubiquitinated CIP2A protein.

### 3.4 | CIP2A is associated with poor survival and can partially reverse the inhibitory effects of TP53TG1 in GC

We assessed CIP2A protein expression in 82 pairs of matched GC cancer tissues and normal tissues from the First Affiliated Hospital of Sun Yat-sen University. We found that CIP2A protein expression was elevated in cancer tissues (Figure 4A,B) and that high CIP2A expression correlated with significantly worse overall survival (Figure 4C). We also found that CIP2A protein expression was elevated in cancer tissues compared with normal gastric tissues in Human Protein Atlas data and was associated with poor prognosis (Figure S4A,B).

To determine whether CIP2A plays a crucial role in the TP53TG1-mediated regulation of GC growth and metastasis, proliferation and invasion abilities were examined in GC cells overexpressing CIP2A and TP53TG1. CCK-8 and colony formation assays showed that the TP53TG1-induced suppression of GC cell proliferation was partially reversed when CIP2A expression was increased (Figure 4D,E and Figure S4C,D). Transwell assays revealed that TP53TG1-mediated suppression of cell migration and invasion was partially reversed in cells cotransfected with TP53TG1 and CIP2A (Figure 4F,G). In addition, concomitant overexpression of TP53TG1 and CIP2A partially counteracted the effects of TP53TG1 on AKT Thr308 and Ser473 phosphorylation in MKN28 and BGC823 cells (Figure 4H). Based on these results, CIP2A is responsible for TP53TG1-mediated GC cell growth and progression.

### 3.5 | TP53TG1 suppresses the progression of GC by attenuating the PI3K/AKT pathway

The PI3K/AKT pathway has been reported to participate in cell proliferation, cell migration and cancer metastasis.<sup>20</sup> As TP53TG1 mediates tumor suppressor activity by attenuating PI3K/AKT, we performed rescue assays to further prove it. The AKT inhibitor MK2206 greatly inhibited TP53TG1 knockdown-induced GC cell growth, as shown by CCK-8 and colony formation assays (Figure 5A–C). Meanwhile, we observed that MK2206 also suppressed the migration and invasion of TP53TG1 knockdown-induced cells (Figure 5D, E). In addition, Western blotting showed that MK2206 inhibited AKT Thr308 and Ser473 phosphorylation (Figure 5F). Altogether, these data show that the PI3K/AKT pathway is essential for mediating TP53TG1 tumor-inhibiting activity.

### 3.6 | TP53TG1 suppresses the progression of GC in vivo

To further study the roles of TP53TG1 in vivo, we established subcutaneous tumor and lung metastasis models in nude mice (Figure 6A). Compared with that in the control group, the tumor growth rate was decreased in the TP53TG1-overexpressing group. Tumor weight and volume were also significantly reduced in the TP53TG1-overexpressing group (Figure 6B,C). Hematoxylin and eosin (HE) staining was performed to identify tumors (Figure 6D left panel). More importantly, the expression of Ki67, CIP2A, and BAX was negatively correlated with the TP53TG1 level in these tumor tissues, while PP2A expression was positively associated with the TP53TG1 level (Figure 6D). TUNEL apoptosis assay with xenograft tumor samples revealed that TP53TG1 facilitated the apoptosis of GC cells in vivo (Figure 6D right panel). These results suggested a potential inhibitory effect of the TP53TG1 on the proliferation of GC cells in vivo. Furthermore, by injecting stably transfected GC cells into the tail vein of nude mice, TP53TG1 dramatically inhibited the development of pulmonary metastasis (Figure 6E,F).

### 3.7 | ALKBH5 regulates TP53TG1 stability through m6A modification

Recent advancements in understanding tumor epigenetic regulation have shed light on the involvement of the m6A modification in lncRNA functions. According to the online bioinformatics database m6Avar, there are five RRACU m6A sequence motifs in the exon region of TP53TG1 (on chr7 at 87341611(-), 87341669(-), 87345112(-), 87345112(-), and 87345247(-)). We then speculated whether m6A was associated with TP53TG1 downregulation in GC cells. Compared with the normal GC cell line GES-1, the m6A level of TP53TG1 was lower in MKN28, BGC823, HGC27, MGC803, MKN45, and AGS cells, indicating that m6A may be involved in TP53TG1 downregulation (Figure 7A). The sequence motifs in m6A peaks were identified with the MEME Suite (<https://meme-suite.org/meme/>) (Figure 7B).

ALKBH5 is a crucial m6A methyltransferase and has been reported to be involved in GC development.<sup>21</sup> ALKBH5 has been previously found to be elevated in the cancer tissues of patients and play pro-oncogenic roles.<sup>22</sup> RT-qPCR results indicated that the ALKBH5 expression level was negatively correlated with the level of TP53TG1 in the 82 GC tissue samples (Figure S5A). To explore the effects of ALKBH5 on TP53TG1 stability in GC cells, we

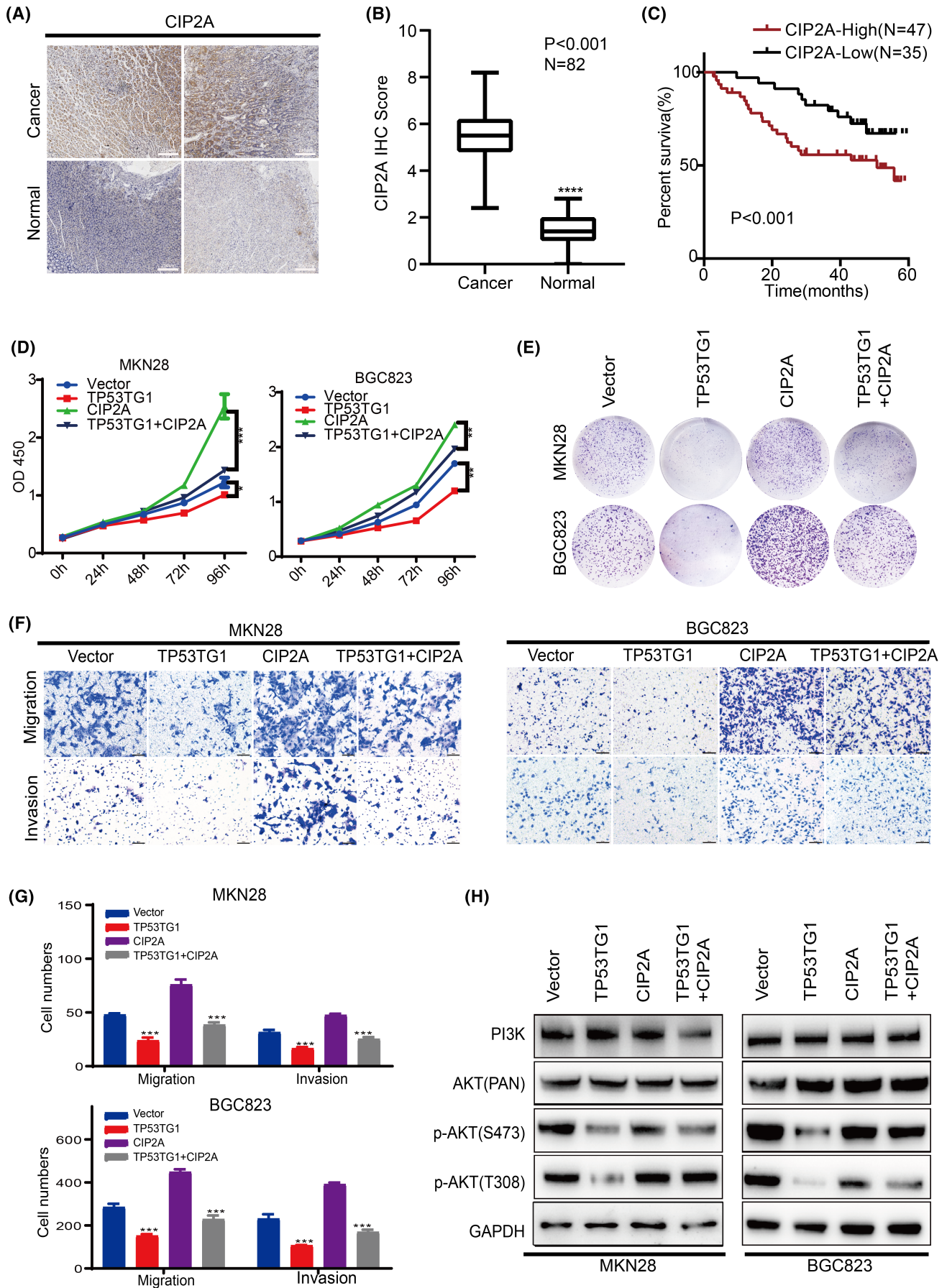


**FIGURE 4** CIP2A partially reversed the tumor inhibitory function of TP53TG1 in gastric cancer (GC) cells. (A) Representative image of CIP2A immunohistochemistry (IHC) staining showing 82 matched normal and GC tissues. (B) IHC score shows the expression of CIP2A in matched normal and GC tissues. (C) Kaplan-Meier analysis revealed that high CIP2A expression in GC patients was significantly correlated with a dismal prognosis. Median histochemical value of CIP2A value (5.6) was used to divide patients into CIP2A-high and CIP2A-low groups. (D) CIP2A reversed the inhibitory effects of TP53TG1 on the proliferation of GC cells, as assessed by CCK-8 assay. (E) CIP2A reversed the inhibitory effects of TP53TG1 on the colony formation of GC cells. (F) Transwell assays showing that the TP53TG1-mediated inhibition of migration and invasion was rescued by CIP2A in GC cells. (G) Statistical analysis of the migration and invasion assays is shown. (H) Western blotting showing that the TP53TG1-mediated inhibition of the PI3K/AKT signaling pathway was rescued by CIP2A in GC cells.

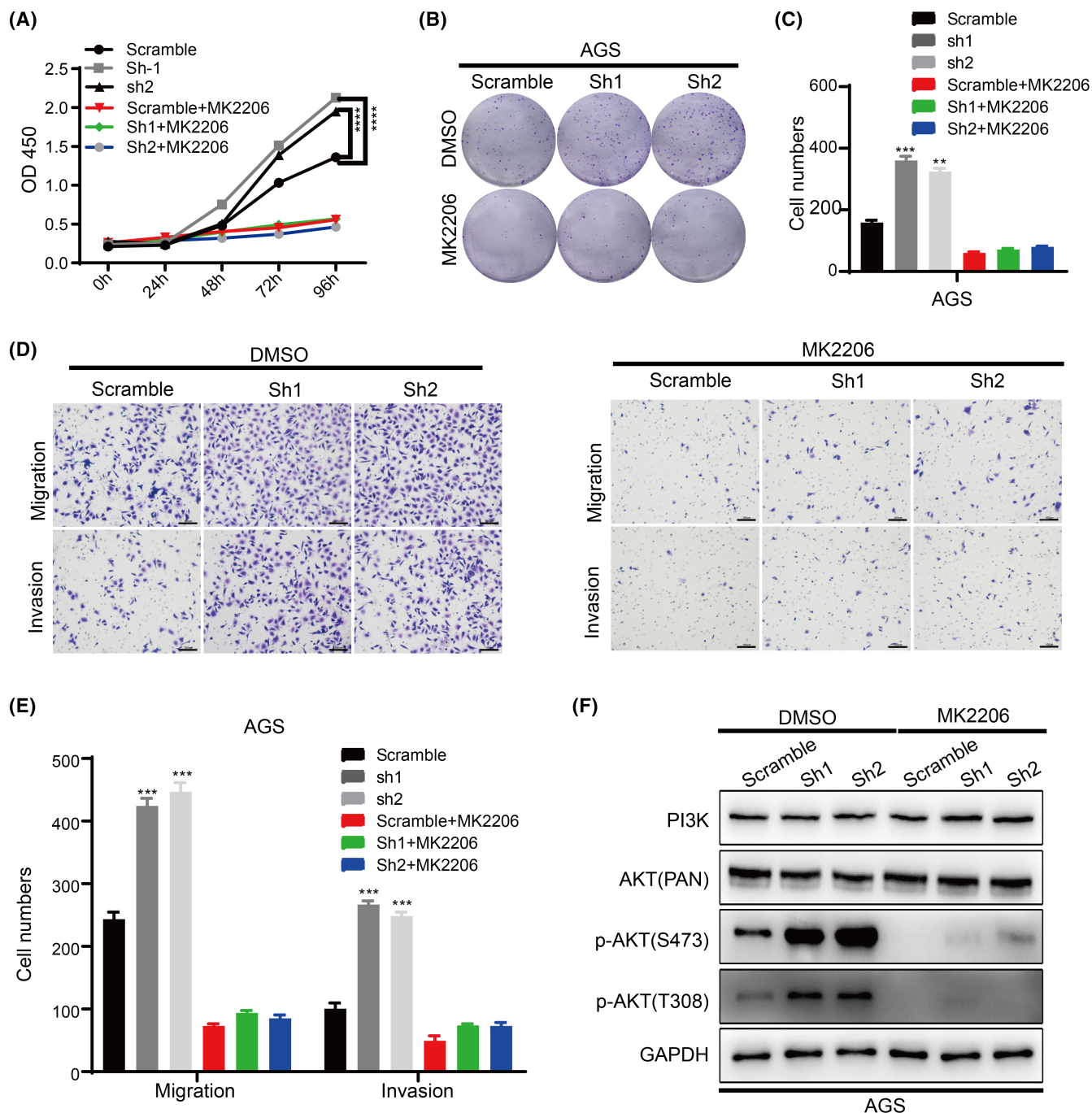


**FIGURE 5** TP53TG1 suppressed the progression of gastric cancer (GC) by attenuating the PI3K/AKT pathway. (A-C) Proliferation assays of the knockdown-induced AGS cells treated with DMSO or an AKT inhibitor MK2206. (D-E) Transwell assays of the knockdown-induced AGS cells treated with DMSO or AKT inhibitor MK2206. (F) Western blotting detecting the protein levels of the PI3K/AKT pathway on the knockdown-induced AGS cells treated with DMSO or AKT inhibitor MK2206

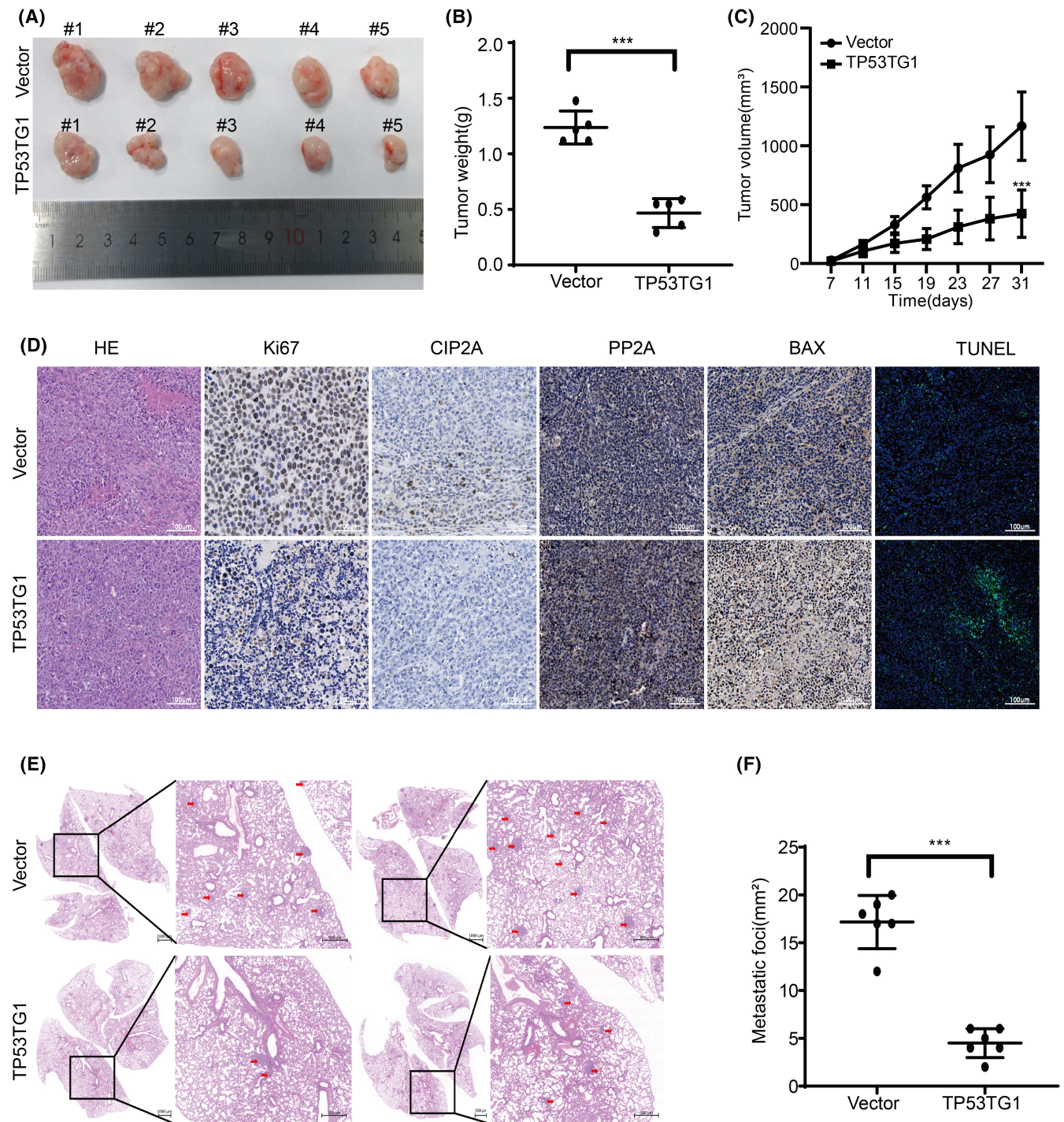


**FIGURE 6** TP53TG1 suppressed the progression and metastasis of gastric cancer (GC) in vivo. (A) Representative images of subcutaneous xenograft tumors after injection of TP53TG1 stably overexpressing or negative control GC cells. (B, C) Weights and volumes of subcutaneous tumors. (D) Representative images of H&E and immunohistochemistry (IHC) staining with antibodies against Ki67, CIP2A, PP2A, and BAX in subcutaneous xenograft specimens. TUNEL apoptosis assay showing the apoptotic cells in subcutaneous tumors. (E) Representative H&E staining images of lung metastasis models of TP53TG1 overexpression groups and control group. (F) Statistical analysis of numbers of metastatic nodules in the lungs.

stably knocked down ALKBH5 with a lentivirus vector in MKN28 and BGC823 cell lines. Western blotting assays and RT-qPCR verified the knockdown efficiency (Figure 7C,D). Compared with that in the control group, the m6A level of TP53TG1 was higher in ALKBH5-silenced GC cells (Figure 7E,F). Besides, we found that

ALKBH5 silencing was associated with upregulated TP53TG1 expression (Figure 7G). RIP analysis demonstrated that TP53TG1 was significantly enriched by the ALKBH5 antibody in both MKN28 and BGC823 cell lines (Figure 7H). We then treated GC cells with actinomycin D to block transcription and found that ALKBH5

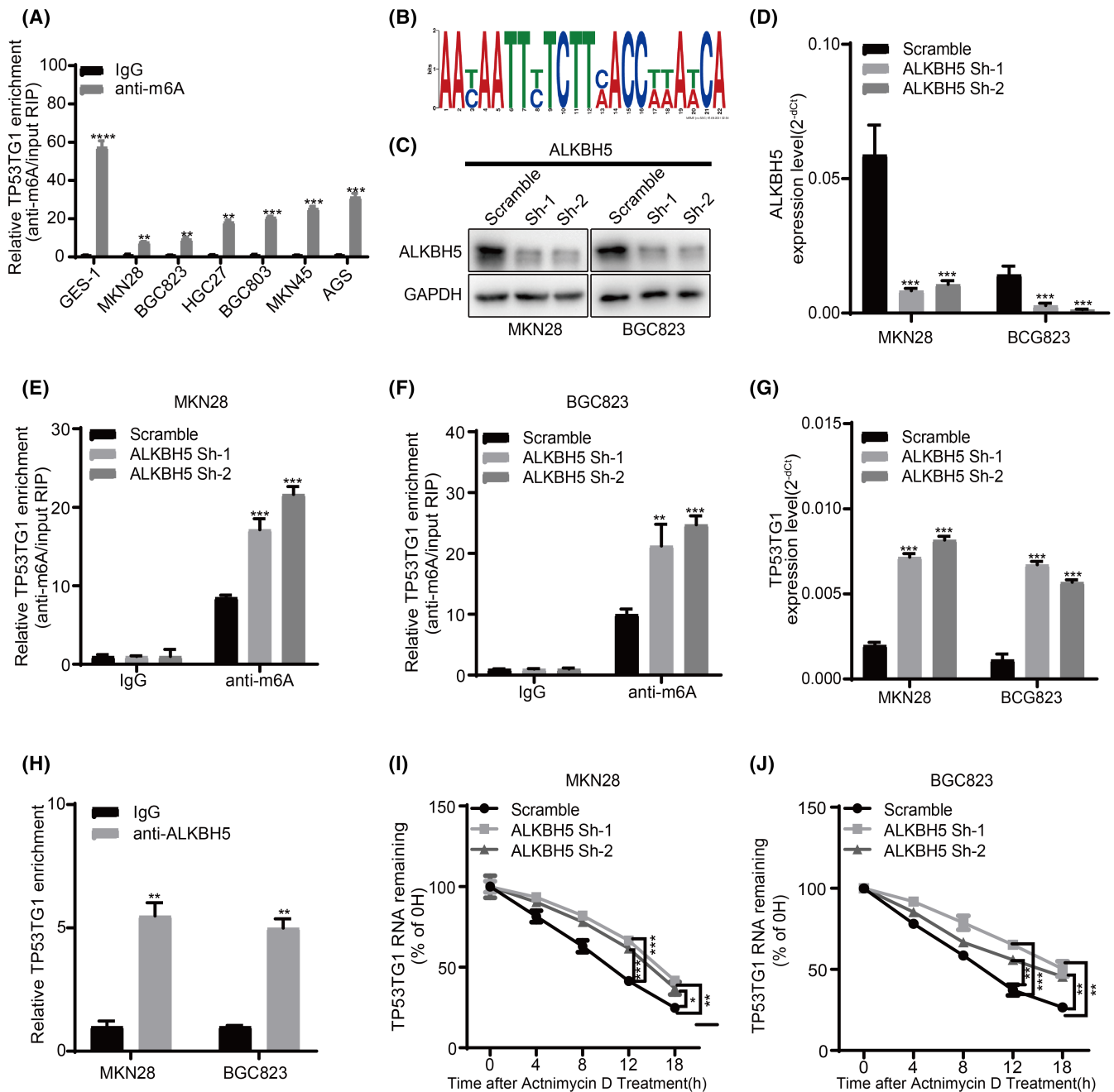


**FIGURE 7** ALKBH5 silencing upregulated TP53TG1 expression by m6A modification. (A) m6A RIP-qPCR analysis of m6A modification level of TP53TG1 in gastric cancer (GC) cells. (B) Sequence motifs in m6A peaks identified using the MEME Suite tool (<https://meme-suite.org/meme/>). (C, D) Western blotting and RT-qPCR analysis were performed to detect ALKBH5 levels in GC cells. (E, F) The m6A modification level of TP53TG1 was examined in ALKBH5 knockdown or negative control cells. (G) The expression of TP53TG1 was examined in ALKBH5 knockdown or negative control cells. (H) RIP-qPCR assay with anti-ALKBH5 or IgG to detect the enrichment of TP53TG1 in GC cells. (I, J) GC cells treated with actinomycin D for the indicated times; the level of TP53TG1 was examined by RT-qPCR.

silencing significantly increased the half-life of TP53TG1 in MKN28 and BGC823 cells (Figure 7I,J). We also overexpressed ALKBH5 with a lentivirus vector in AGS cells (Figure S5B,C). We found that ALKBH5 overexpression dramatically decreased m6A modification level of TP53TG1 in GC cells (Figure S5D). In addition, we found that ALKBH5 overexpression was associated with decreased TP53TG1 expression (Figure S5E). TP53TG1 was also significantly enriched

in the anti-ALKBH5 group in the AGS cell line according to the RIP analysis (Figure S5F). We also found that ALKBH5 overexpression significantly decreased the half-life of TP53TG1 in the AGS cell line by using actinomycin D to block its transcription (Figure S5G). These results suggested that ALKBH5-mediated m6A is associated with the downregulation of TP53TG1 in GC cells, probably by regulating TP53TG1 transcript stability.

## 4 | DISCUSSION

Long noncoding RNAs are newly discovered players in the cancer paradigm, with regulatory functions in both carcinogenic and tumor suppressive pathways,<sup>23</sup> including those in GC.<sup>24,25</sup> Recent reports have demonstrated that TP53TG1 exerts oncogenic or tumor-suppressing functions in different cancers. TP53TG1 plays a cancer-promoting effect in pancreatic cancer and glioma,<sup>26,27</sup> but it exerts an antitumor effect in colorectal cancer, non-small cell lung cancer, and liver cancer.<sup>28-30</sup> In this study, we found that TP53TG1 expression was significantly downregulated and exerted tumor-suppressing functions in GC.

Previous studies have shown that the mechanism of lncRNAs in human diseases is linked to their cellular location.<sup>7</sup> lncRNAs located in the nucleus mainly interact with chromatin and regulate transcription and RNA processing.<sup>31</sup> The main biological functions of those located in the cytoplasm mainly include the stabilization of mRNAs,<sup>32</sup> participation in the posttranscriptional regulation of mRNAs as competing endogenous RNAs (ceRNAs),<sup>33</sup> and protein modification processes.<sup>34,35</sup> The aberrant expression of lncRNAs exerts diverse effects on the pathogenesis of cancers through various mechanisms.<sup>36</sup> In pancreatic cancer, TP53TG1 promotes the growth and progression of pancreatic ductal carcinoma by competitively binding to miR-96 and regulating the KRAS expression,<sup>26</sup> while in non-small cell lung cancer, TP53TG1 increases the sensitivity to cisplatin by regulating the miR-18a/PTEN axis.<sup>29</sup> Cytoplasmic lncRNAs also can affect the expression, activity, and/or cell location of proteins by binding to them.<sup>37</sup> In liver cancer, TP53TG1 affects the WNT/ $\beta$ -catenin signaling pathway by binding to PRDX4.<sup>30</sup> The epigenetic inactivation of TP53TG1 abates the transcriptional suppression of YBX1-targeted growth-promoting genes, and contributes to the generation of chemoresistance in gastrointestinal cancer.<sup>28</sup> Furthermore, TP53TG1 under glucose deprivation may promote cell proliferation and migration by influencing the expression of glucose metabolism-related genes in glioma.<sup>27</sup> Herein, our results indicated that TP53TG1 binds to CIP2A and regulates its subsequent ubiquitin-mediated degradation, thus inhibiting the activation of the PI3K/AKT pathway. CIP2A is a human oncoprotein that can promote cancer cell proliferation, anchorage-independent cell growth, and resistance to apoptosis.<sup>38</sup> The PI3K/Akt signaling pathway is activated in an extensive variety of tumor types and drives cancer cell proliferation and survival.<sup>39</sup> The CIP2A complex inhibits PP2A activity to regulate the AKT pathway by dephosphorylating both the Thr308 and Ser 473 residues in Akt in a context-dependent manner.<sup>40</sup> In this study, we found that CIP2A overexpression can partially reverse the inhibition of the PI3K/AKT pathway induced by TP53TG1, enhancing AKT phosphorylation/activation in GC cells.

TP53TG1 is an important tumor suppressor in cancer, but the reason for its decreased expression is not clear. Diaz-Lagares A et al demonstrated that the low expression of TP53TG1 may be related to DNA methylation and the regulation of TP53 transcription at the DNA level.<sup>28</sup> In recent years, m6A modification has been

shown to have significant effects in regulating all stages of the RNA life cycle.<sup>41</sup> The abnormality of the enzyme or reading protein that regulates m6A methylation modification will lead to the occurrence of many diseases. For cancers, m6A methyltransferase catalyzes the methylation of oncogene/suppressor RNA, and then a series of m6A reading proteins recognize these m6A methylation modifications, and upregulate or downregulate the oncogene/suppressor gene expression, playing a corresponding role in promoting or suppressing cancer.<sup>42</sup> ALKBH5 has been shown to interact with SOX2, causing SOX2 mRNA demethylation, and resulting in increased SOX2 expression.<sup>43</sup> Here, we analyzed data from a bioinformatics database and MeRIP experiment results and found that m6A modification was enriched on TP53TG1 in GC cells. In addition, ALKBH5 negatively regulated the m6A modification of TP53TG1, thereby affecting the stability of its RNA. Thus, our results indicate that the decrease of TP53TG1 in GC may be attributed to m6A modification.

In summary, our study revealed that TP53TG1 binds to CIP2A and promotes its ubiquitination and then inhibits the activation of the PI3K/AKT pathway. We also highlighted that ALKBH5, a m6A recognition molecule, reduces the m6A modification level of TP53TG1, thus affecting the stability of RNA. The above findings provide a potential molecular target for the clinical treatment of GC.

## ACKNOWLEDGEMENTS

The authors thank GeneCopoeia(USA) for plasmids construction and Guangzhou Gene Denovo Biotechnology Co.,Ltd(China) for the support of RNA-seq.

## FUNDING INFORMATION

This study was supported by the National Natural Science Foundation of China (81871915 and 81672343) and the Natural Science Foundation of Guangdong, China (2022A1515012140, 2017A030313570, 2018A030313543).

## CONFLICT OF INTEREST

The authors have no conflict of interest.

## ETHICS STATEMENT

All human samples were obtained with informed consent from patients with gastric cancer. Ethical consent was granted from the Ethical Committee Review Board of the First Affiliated Hospital of Sun Yat-sen University. The animal study was reviewed and approved by the Ethical Committee Review Board of the First Affiliated Hospital of Sun Yat-sen University (permit number: No. [2020]035).

## ORCID

Jianbo Xu  <https://orcid.org/0000-0001-9143-168X>

## REFERENCES

1. Sung H, Ferlay J, Siegel RL, et al. Global Cancer Statistics 2020: GLOBOCAN estimates of incidence and mortality worldwide for 36 cancers in 185 countries. *CA Cancer J Clin.* 2021;71(3):209-249.

2. Wang FH, Zhang XT, Li YF, et al. The Chinese Society of Clinical Oncology (CSCO): clinical guidelines for the diagnosis and treatment of gastric cancer, 2021. *Cancer Commun (Lond)*. 2021;41(8):747-795.
3. Cai Q, Shi P, Yuan Y, et al. Inflammation-associated senescence promotes *Helicobacter pylori*-induced atrophic gastritis. *Cell Mol Gastroenterol Hepatol*. 2021;11(3):857-880.
4. Wang FH, Shen L, Li J, et al. The Chinese Society of Clinical Oncology (CSCO): clinical guidelines for the diagnosis and treatment of gastric cancer. *Cancer Commun (Lond)*. 2019;39(1):10.
5. Dragomir MP, Kopetz S, Ajani JA, Calin GA. Non-coding RNAs in GI cancers: from cancer hallmarks to clinical utility. *Gut*. 2020;69(4):748-763.
6. Anastasiadou E, Jacob LS, Slack FJ. Non-coding RNA networks in cancer. *Nat Rev Cancer*. 2018;18(1):5-18.
7. Statello L, Guo CJ, Chen LL, Huarte M. Gene regulation by long non-coding RNAs and its biological functions. *Nat Rev Mol Cell Biol*. 2021;22(2):96-118.
8. Gil N, Ulitsky I. Regulation of gene expression by cis-acting long non-coding RNAs. *Nat Rev Genet*. 2020;21(2):102-117.
9. Romero-Barrios N, Legascue MF, Benhamed M, Ariel F, Crespi M. Splicing regulation by long noncoding RNAs. *Nucleic Acids Res*. 2018;46(5):2169-2184.
10. Liu HT, Liu S, Liu L, Ma RR, Gao P. EGR1-mediated transcription of lncRNA-HNF1A-AS1 promotes cell-cycle progression in gastric cancer. *Cancer Res*. 2018;78(20):5877-5890.
11. Zhao Y, Liu Y, Lin L, et al. The lncRNA MACC1-AS1 promotes gastric cancer cell metabolic plasticity via AMPK/Lin28 mediated mRNA stability of MACC1. *Mol Cancer*. 2018;17(1):69.
12. Chen Y, Lin Y, Shu Y, He J, Gao W. Interaction between N(6)-methyladenosine (m(6)A) modification and noncoding RNAs in cancer. *Mol Cancer*. 2020;19(1):94.
13. Wang T, Kong S, Tao M, Ju S. The potential role of RNA N6-methyladenosine in cancer progression. *Mol Cancer*. 2020;19(1):88.
14. Batista PJ, Molinie B, Wang J, et al. m(6)A RNA modification controls cell fate transition in mammalian embryonic stem cells. *Cell Stem Cell*. 2014;15(6):707-719.
15. Geula S, Moshitch-Moshkovitz S, Dominissini D, et al. Stem cells. m6A mRNA methylation facilitates resolution of naïve pluripotency toward differentiation. *Science*. 2015;347(6225):1002-1006.
16. Zhu L, Zhu Y, Han S, et al. Impaired autophagic degradation of lncRNA ARHGAP5-AS1 promotes chemoresistance in gastric cancer. *Cell Death Dis*. 2019;10(6):383.
17. Zhang J, Guo S, Piao HY, et al. ALKBH5 promotes invasion and metastasis of gastric cancer by decreasing methylation of the lncRNA NEAT1. *J Physiol Biochem*. 2019;75(3):379-389.
18. Wang Z, Shu H, Wang Z, et al. Loss expression of PHLPP1 correlates with lymph node metastasis and exhibits a poor prognosis in patients with gastric cancer. *J Surg Oncol*. 2013;108(7):427-432.
19. Dongre A, Weinberg RA. New insights into the mechanisms of epithelial-mesenchymal transition and implications for cancer. *Nat Rev Mol Cell Biol*. 2019;20(2):69-84.
20. Hua H, Zhang H, Chen J, Wang J, Liu J, Jiang Y. Targeting Akt in cancer for precision therapy. *J Hematol Oncol*. 2021;14(1):128.
21. Hu Y, Gong C, Li Z, et al. Demethylase ALKBH5 suppresses invasion of gastric cancer via PKMYT1 m6A modification. *Mol Cancer*. 2022;21(1):34.
22. Zhang S, Zhao BS, Zhou A, et al. m(6)A demethylase ALKBH5 maintains tumorigenicity of glioblastoma stem-like cells by sustaining FOXM1 expression and cell proliferation program. *Cancer Cell*. 2017;31(4):591-606.e6.
23. Sánchez Y, Huarte M. Long non-coding RNAs: challenges for diagnosis and therapies. *Nucleic Acid Ther*. 2013;23(1):15-20.
24. Kong F, Deng X, Kong X, et al. ZFPM2-AS1, a novel lncRNA, attenuates the p53 pathway and promotes gastric carcinogenesis by stabilizing MIF. *Oncogene*. 2018;37(45):5982-5996.
25. Zhang JX, Chen ZH, Chen DL, et al. LINC01410-miR-532-NCF2-NF- $\kappa$ B feedback loop promotes gastric cancer angiogenesis and metastasis. *Oncogene*. 2018;37(20):2660-2675.
26. Zhang Y, Yang H, Du Y, et al. Long noncoding RNA TP53TG1 promotes pancreatic ductal adenocarcinoma development by acting as a molecular sponge of microRNA-96. *Cancer Sci*. 2019;110(9):2760-2772.
27. Chen X, Gao Y, Li D, Cao Y, Hao B. lncRNA-TP53TG1 participated in the stress response under glucose deprivation in glioma. *J Cell Biochem*. 2017;118(12):4897-4904.
28. Diaz-Lagares A, Crujeiras AB, Lopez-Serra P, et al. Epigenetic inactivation of the p53-induced long noncoding RNA TP53 target 1 in human cancer. *Proc Natl Acad Sci U S A*. 2016;113(47):E7535-e44.
29. Xiao H, Liu Y, Liang P, et al. TP53TG1 enhances cisplatin sensitivity of non-small cell lung cancer cells through regulating miR-18a/PTEN axis. *Cell Biosci*. 2018;8:23.
30. Chen B, Lan J, Xiao Y, et al. Long noncoding RNA TP53TG1 suppresses the growth and metastasis of hepatocellular carcinoma by regulating the PRDX4/ $\beta$ -catenin pathway. *Cancer Lett*. 2021;513:75-89.
31. Shin TJ, Lee KH, Cho JY. Epigenetic mechanisms of lncRNAs binding to protein in carcinogenesis. *Cancers (Basel)*. 2020;12(10):2952.
32. Liu X, Li D, Zhang W, Guo M, Zhan Q. Long non-coding RNA gadd7 interacts with TDP-43 and regulates Cdk6 mRNA decay. *EMBO J*. 2012;31(23):4415-4427.
33. Salmena L, Poliseno L, Tay Y, Kats L, Pandolfi PP. A ceRNA hypothesis: the Rosetta Stone of a hidden RNA language? *Cell*. 2011;146(3):353-358.
34. Wang P, Xue Y, Han Y, et al. The STAT3-binding long noncoding RNA lnc-DC controls human dendritic cell differentiation. *Science*. 2014;344(6181):310-313.
35. Liu B, Sun L, Liu Q, et al. A cytoplasmic NF- $\kappa$ B interacting long non-coding RNA blocks I $\kappa$ B phosphorylation and suppresses breast cancer metastasis. *Cancer Cell*. 2015;27(3):370-381.
36. Fang Y, Fullwood MJ. Roles, functions, and mechanisms of long non-coding RNAs in cancer. *Genomics Proteomics Bioinformatics*. 2016;14(1):42-54.
37. Wang Z, Yang B, Zhang M, et al. lncRNA epigenetic landscape analysis identifies EPIC1 as an oncogenic lncRNA that interacts with MYC and promotes cell-cycle progression in cancer. *Cancer Cell*. 2018;33(4):706-20.e9.
38. Soofiyan SR, Hejazi MS, Baradaran B. The role of CIP2A in cancer: a review and update. *Biomed Pharmacother*. 2017;96:626-633.
39. Yang Q, Jiang W, Hou P. Emerging role of PI3K/AKT in tumor-related epigenetic regulation. *Semin Cancer Biol*. 2019;59:112-124.
40. Wang J, Okkeri J, Pavic K, et al. Oncoprotein CIP2A is stabilized via interaction with tumor suppressor PP2A/B56. *EMBO Rep*. 2017;18(3):437-450.
41. Ma S, Chen C, Ji X, et al. The interplay between m6A RNA methylation and noncoding RNA in cancer. *J Hematol Oncol*. 2019;12(1):121.
42. Oerum S, Meynier V, Catala M, Tisné C. A comprehensive review of m6A/m6Am RNA methyltransferase structures. *Nucleic Acids Res*. 2021;49(13):7239-7255.
43. Liu B, Zhou J, Wang C, et al. lncRNA SOX2OT promotes temozolomide resistance by elevating SOX2 expression via ALKBH5-mediated epigenetic regulation in glioblastoma. *Cell Death Dis*. 2020;11(5):384.
44. Amin MB, Greene FL, Edge SB, et al. The eighth edition AJCC cancer staging manual: Continuing to build a bridge from a

population-based to a more "personalized" approach to cancer staging. *CA Cancer J Clin.* 2017;67(2):93-99.

#### SUPPORTING INFORMATION

Additional supporting information can be found online in the Supporting Information section at the end of this article.

**How to cite this article:** Fang D, Ou X, Sun K, et al. m6A modification-mediated lncRNA TP53TG1 inhibits gastric cancer progression by regulating CIP2A stability. *Cancer Sci.* 2022;113:4135-4150. doi: [10.1111/cas.15581](https://doi.org/10.1111/cas.15581)